Evidence for an Elongated (>60 Ion Skin Depths) Electron Diffusion Region during Fast Magnetic Reconnection

T. D. Phan,[1] J. F. Drake,[1,2] M. A. Shay,[3] F. S. Mozer,[1] and J. P. Eastwood[1]
[1]*Space Sciences Laboratory, University of California, Berkeley, California 94720, USA*
[2]*University of Maryland, College Park, Maryland, 20742, USA*
[3]*Department of Physics and Astronomy, University of Delaware, Newark, Delaware 19716, USA*
(Received 9 October 2007; published 21 December 2007)

Observations of an extremely elongated electron diffusion region occurring during fast reconnection are presented. Cluster spacecraft *in situ* observations of an expanding reconnection exhaust reveal a broad current layer (~10 ion skin depths thick) supporting the reversal of the reconnecting magnetic field together with an intense current embedded at the center that is due to a super-Alfvénic electron outflow jet with transverse scale of ~9 electron skin depths. The electron jet extends at least 60 ion skin depths downstream from the X-line.

DOI: 10.1103/PhysRevLett.99.255002 PACS numbers: 94.30.cp, 52.35.Vd, 94.30.cj

Magnetic reconnection drives explosive phenomena in laboratory and astrophysical plasma. The process is thought to be initiated in a small diffusion region around a magnetic X-line, but its consequences are large scale. Understanding the structure of the diffusion region and its role in controlling the rate at which magnetic energy is converted into particle energy remains a key scientific challenge. Specifically, because of the continuity of flow into and out of the diffusion region, elongated diffusion regions lead to reduced rates of reconnection. Early full particle simulations [1–3] predicted a short electron diffusion region, characterized by a strong out-of-plane electron current, with a width of a few c/ω_{pe} (with c/ω_{pe} the electron skin depth) and a length of $5-10\ c/\omega_{pe}$. The modest (roughly 1 to 10) aspect ratio of the diffusion region led to fast reconnection. In contrast, open-boundary simulations[4] suggested that the length of the out-of-plane electron current layer is much longer ($\gg$ the ion skin depth c/ω_{pi}) such that the reconnection rate is significantly reduced. However, recent full particle simulations in larger simulation domains[5,6] revealed the existence of an extended electron diffusion region but with fast reconnection. In the new model, the out-of-plane current is spatially localized to within a few c/ω_{pi} of the X-line [Fig. 1(a)] and does not lengthen with time as seen in previous smaller-scale open-boundary simulations[4]. This inner electron region is connected to a long super-Alfvénic electron jet that extends at least $15\ c/\omega_{pi}$ from the X-line [Fig. 1(b)] and is not frozen to the magnetic field [Fig. 1(e)]. Central to the model is that while the electron jet remains highly collimated along its entire extent, the electrons also form a laterally expanding outflow exhaust that allows reconnection to be fast. These predictions have not yet been verified in space or the laboratory. Thus, it is critical to determine observationally whether such a long electron outflow jet exists and whether it throttles reconnection.

In this Letter, we present observations of a super-Alfvénic electron outflow jet inside a current sheet undergoing fast reconnection. The oblique trajectory of the spacecraft through the diffusion region enabled the first definitive determination of the length of the electron diffusion region, which extended at least $60\ c/\omega_{pi}$ downstream of the X-line, far exceeding what is seen in current simulations.

On 2003-01-14, the Cluster-1 spacecraft detected the passage of a large-scale, nearly-planar current sheet at ~06:12:00 UT in the magnetosheath region downstream of the Earth's bow shock [7]. The basic elements of the event in the current sheet (LMN) coordinate system are summarized in Fig. 2. The previous study established the large-scale context of this reconnection exhaust, its geometry, motion, and the measured reconnection rate based on the plasma and electric field measurements (Fig. 3). The magnetic field rotation across the entire magnetic field reversal was 162° [Fig. 3(a)]. The $7nT$ guide field [B_M just outside the current sheet in Fig. 3(a)] was 15% of the reconnecting field B_L. There was a slight (~10%) density asymmetry across the current sheet. The external magnetosheath flow tangential to the current sheet was −80 km/s (−100 km/s) along the L direction and −100 km/s (−140 km/s) along the M direction on the leading (trailing) edge of the current sheet [Fig. 3(b)]. The rather weak asymmetries in the plasma and magnetic fields between the two inflow regions mean that the reconnection configuration was nearly symmetric. Here, we focus on the high-time resolution observations of the ion and electron-scale structures of the reconnection layer. For simplicity and for consistency, the normalization used in the following discussions will be based on the plasma and field parameters in the inflow region on the trailing edge (upper edge in Fig. 2) of the current sheet. In the analysis, we will assume that the reconnection X-line is stationary in the rest frame of magnetosheath flow (on the trailing edge side), i.e., the

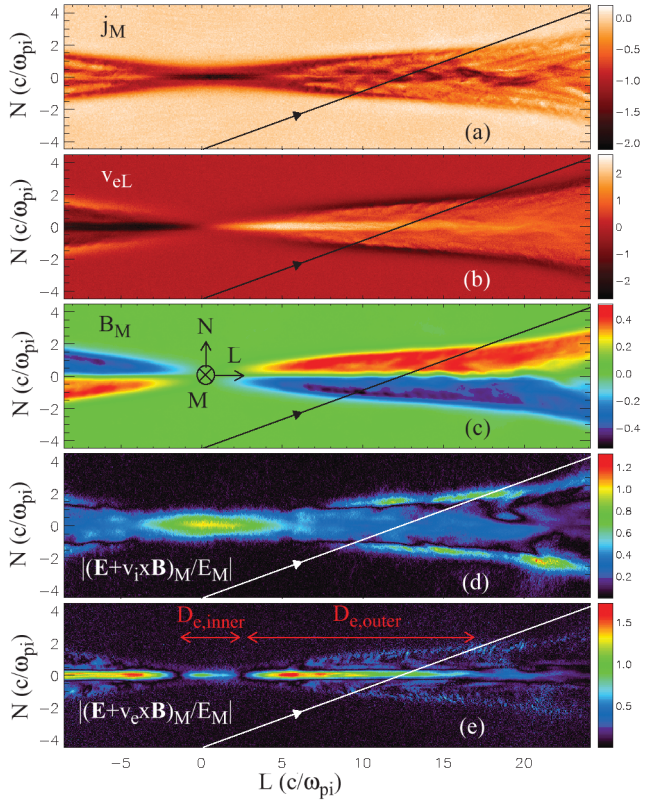

FIG. 1 (color). Results from simulations with 91.6 $c/\omega_{pi} \times$ 45.8 c/ω_{pi} and $m_i/m_e = 25$ in the $N - L$ plane[5]. The LMN coordinate system is defined with N along the current sheet normal, M along the X-line direction, and L along the outflow direction. (a) the out-of-plane current j_M, (b) the electron outflow velocity v_{eL}, (c) the Hall magnetic field B_M, and the frozen-in conditions for (d) the ions and (e) the electrons. Parameters are normalized to the inflow values. Simulations have been unable to establish the limiting size of this jet since it appears to lengthen as the simulation domain is extended. The oblique line is the virtual spacecraft trajectory. The low mass ratio, which permits large-scale simulations, displays the same essential physics as higher mass-ratio simulations [5].

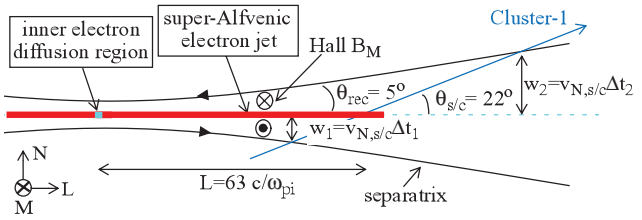

FIG. 2 (color). Schematic of the Cluster-1 crossing of an elongated outer electron diffusion region in which the electron flow is super-Alfvénic. The oblique trajectory of the spacecraft through the exhaust at an angle $\theta_{s/c}$ results in an asymmetry in the measured duration of the Hall magnetic and electric fields below and above the current sheet midplane. Based on this asymmetry, the reconnection exhaust wedge half-angle θ_{rec} (i.e., the reconnection rate) as well as the distance from the X-line of the intersection of the spacecraft with the electron jet can be determined.

X-line moves at $v_L = -100$ km/s in the spacecraft frame. This important assumption will be validated by the results of the analysis.

Figure 3(b) shows the presence of an accelerated ion flow v_L seen throughout the current sheet (between the two vertical dashed lines). The peak velocity of the ion jet was ~80 km/s in the spacecraft frame and 180 km/s in the X-line frame. Thus, the ion outflow speed was ~78% of the inflow Alfvén speed, where $v_{A,inflow} \sim 230$ km/s, based on a density of ~18 cm^{-3} and B_L of $45nT$ in the inflow region. Figure 3(b) also shows that the current sheet convects with the magnetosheath flow past the spacecraft at a normal velocity of $v_{N,s/c} \sim -40$ km/s. The constant motion of the magnetosheath current sheet past the spacecraft is crucial for translating the time series to a spatial profile. Superimposed on the current sheet normal motion is a reconnection inflow $v_{n,rec}$ of ~15 km/s from the two sides of the current sheet[7], implying a tangential reconnection electric field $E_M \sim -0.7$ mV/m. The dimensionless reconnection rate $v_{n,rec}/v_{A,inflow}$ was ~7%. The reconnection rate based on the ion inflow was consistent with the directly measured tangential electric field E_M of ~ -0.61 mV/m (averaged over 06:11:40–06:12:20 UT) in the X-line frame [Fig. 3(d)]. The 7% reconnection rate is also comparable to the reconnection rate based on the ratio of the normal magnetic field ($<B_N> \sim -3nT$) to the antiparallel magnetic field (of $45nT$). In addition to the fluid signatures of reconnection in terms of the ion outflow and inflow, Cluster-1 also observed the bipolar Hall magnetic field B_M[8–13] [Fig. 3(a)] and electric field E_N[12,14] [Fig. 3(d)] indicative of the decoupling of the ions from the electrons. The key feature of Fig. 3 is the absence of a gap (i.e., null region) between the positive and negative values of B_M and E_N in the middle of the current sheet (the dotted vertical line). Such a gap would be expected if the spacecraft crossing occurred downstream of the diffusion region [see Fig. 1(c) at $L > 20$ c/ω_{pi}]. Instead, the largest variation of B_M and E_N occurred in the middle of the current sheet [Figs. 3(a) and 4(a)], indicating the presence of an intense current j_L along the outflow direction. An indication that the steep B_M profile is a spatial feature, rather than an artifact of a sudden and brief acceleration of the current sheet normal motion, is the fact that the steepest profile of B_M at the center of the current sheet occurred where the B_L profile was nearly flat.

Because the current sheet convected with the magnetosheath flow at a constant speed $v_{Ns/c} = -40$ km/s, the current density can be estimated from $j_L = \Delta B_M/(\mu_0 v_{Ns/c}\Delta t)$. Figure 4(b) shows the presence of a well-defined current layer (between the two dashed lines) at the center of the reconnection layer, with a peak current of 1 $\mu A/m^2$. This current requires a super-Alfvénic electron jet $v_{eL} = v_{iL} - j_L/eN_i$ [Fig. 4(c)], which reached a speed of ~400 km/s ($1.7v_{A,inflow}$), in the frame of the X-line. This jet was not frozen-in since its perpendicular speed

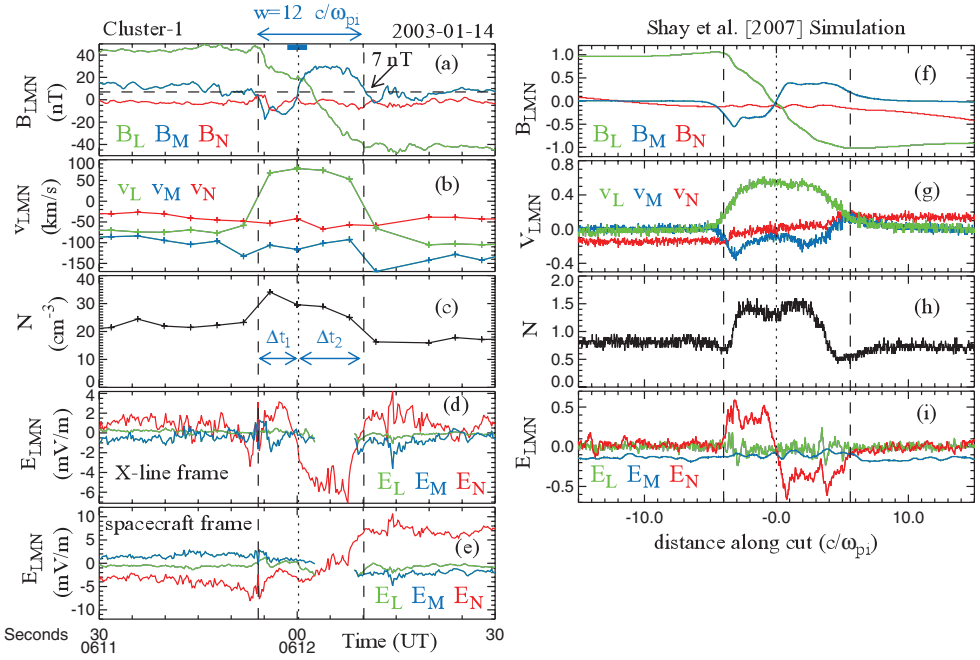

FIG. 3 (color). Cluster-1 crossing of a reconnection exhaust in the vicinity of an X-line and the comparison between the observed and simulated plasma and field profiles. (a) Magnetic field, (b) ion bulk flow, (c) ion density, (d) electric field components in the X-line frame, (e) electric field in the spacecraft frame. The X-line frame was constructed from the spacecraft frame by a translation of $v_L = -100$ km/s, $v_M = -127$ km/s, and $v_N = -40$ km/s based on the ambient magnetosheath flow. The spin-axis component of the electric field E_z was constructed using the $\mathbf{E} \cdot \mathbf{B} = 0$ assumption (when the GSE fields satisfy $|B_{x,y}/B_z| < 2$ and $|B_z| > 2$ to prevent small errors in the measured E_x and E_y from being amplified by small B_z to produce large errors in E_z). Panels (f)–(i) show the corresponding plasma and fields parameters from the simulation along the cut shown in Fig. 1.

(180 km/s) was substantially larger than the $\mathbf{E} \times \mathbf{B}$ drift speed (100 km/s). The width of the electron jet (between the dashed lines in Fig. 4) was ~11 km (~9 c/ω_{pe}). In the broader region outside this super-Alfvénic jet, there was an electron outflow of 200–230 km/s [Fig. 4(c)]. Its perpendicular speed was nearly at the field line speed and ~10% faster than the ion outflow speed. Thus, outside of the jet (but in the ion diffusion region), the electrons are frozen-in. Integrating $N_e v_{eL}$ across the current sheet, we find that 4% of the outflowing electrons were in the super-Alfvénic jet, and 96% were in the broader exhaust region.

The next important question is where the electron jet was detected relative to the X-line. It is possible to estimate this distance because of the oblique trajectory of the spacecraft through the current sheet. Based on the assumption that the X-line convects with the ambient magnetosheath flow, the Cluster-1 trajectory made an angle of $\theta_{s/c} = 22°$ with respect to the symmetry line (light blue dashed line in Fig. 2). The occurrence of this highly oblique trajectory is confirmed by the observed Hall magnetic field B_M [Fig. 3(a)] and electric field E_N [Fig. 3(d)] profiles. The duration Δt_1 (6.1 s) of the negative B_M (from the left vertical dashed line to the dotted line) is much shorter than the duration Δt_2 (9.9 s) of the positive B_M (from the dotted line to the right dashed line), consistent with the spacecraft entering an expanding exhaust much closer to the X-line (where the exhaust is thinner) than where it exited the exhaust.

With the knowledge of the trajectory through the exhaust and the asymmetry in the duration of B_M, we can estimate the exhaust wedge angle and thus the reconnection rate. The reconnection rate is given by $\tan(\theta_{rec}) = \tan(\theta_{s/c})(\Delta t_2 - \Delta t_1)/(\Delta t_2 + \Delta t_1) = 0.09$. The half wedge angle of the exhaust, θ_{rec}, is ~5°. The same answer could have been obtained from the E_N profile as well. The deduced 9% reconnection rate is close to the directly measured reconnection rate of ~7% and provides an important consistency check on the assumed X-line motion.

We now estimate, using the exhaust wedge angle and the spacecraft trajectory, how far downstream of the X-line the spacecraft crossed the electron jet and the two separatrices. The crossing of the electron jet occurred at $L = v_{Ns/c}\Delta t_1[\cot(\theta_{s/c}) + \cot(\theta_{rec})] = 63c/\omega_{pi}$ downstream of the X-line. The crossings of the lower and upper separatrices (see Fig. 2) occurred at $L = 51c/\omega_{pi}$ and $82c/\omega_{pi}$, respectively, from the X-line. The exhaust width at the location where the spacecraft intersected the lower (upper) separatrix was ~10 c/ω_{pi} (~16 c/ω_{pi}). If we had assumed the X-line velocity in the L direction to be −80 km/s (aligned with the magnetosheath flow on the leading edge), the crossing of the electron jet would have occurred at ~50 c/ω_{pi} from the X-line. However, the

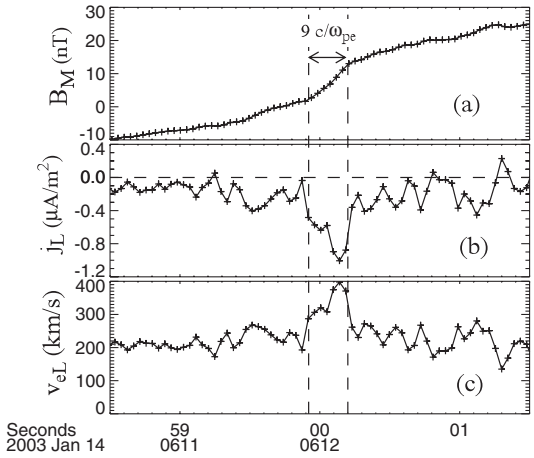

FIG. 4. Detail of the current sheet crossing [interval marked by the blue bar in Fig. 3(a)] showing the presence of an intense current at the center of the current sheet and the implied super-Alfvénic electron outflow. (a) Out-of-plane magnetic field B_M, (b) current density j_L, and (c) electron outflow velocity v_{eL}. The peak electron outflow of ~400 km/s is nearly twice the Alfvén speed.

deduced reconnection rate would have been 12%, further from the directly measured reconnection rates.

We now compare the observations with predictions from recent simulations[5]. Figures 3(f)–3(i) show the plasma and field profiles from the simulation along a trajectory similar to that of the spacecraft (see Fig. 1). The cut through the simulation (which intersects the electron jet at 12 c/ω_{pi} downstream of the X-line) occurred much closer to the X-line than in the observations due to the limitation of the simulation system size. The simulation also assumes symmetric boundary conditions with no guide fields, which is only slightly different from observations. Nevertheless, the agreement between the observed and predicted Hall magnetic and electric field profiles is remarkable. The Hall magnetic and electric field profiles are well reproduced, including the asymmetry in the width of the negative and positive Hall magnetic field B_M regions. There are some slight differences between the observations and simulations. The observed B_M profile is much steeper than in the simulation at the center of the current sheet (the dotted line). This is likely due to the low ion-to-electron mass ratio (25) in the simulation. The observed ion jet (at $0.8v_{A,inflow}$) is faster than the simulated jet speed of $0.6v_A$, which is consistent with the observations being made further downstream of the X-line than in the simulation. The remarkable similarity between the observed and simulated profiles (from a 2-D model) indicates that Cluster-1 did observe the diffusion region structures in the simulation and supports the assumptions of two-dimensionality, time stationarity, and symmetry (about the midplane) used in the analysis of the data.

In summary, the Cluster-1 observations revealed a two-scale structure transverse to a reconnection exhaust, with a broad current layer (width around 535 km or 10 c/ω_{pi}) supporting the reversal of the reconnecting magnetic field B_L and an embedded unfrozen super-Alfvénic electron outflow jet with a width of ~11 km (9 c/ω_{pe}). The electron jet was detected at a distance of 3400 km (63 c/ω_{pi}) downstream from the X-line. In the much broader expanding exhaust region outside the super-Alfvénic electron jet, the electron outflow was nearly Alfvénic and frozen-in, and slightly faster than the ion outflow speed. Only a small fraction (~4%) of the electrons entering the exhaust flow outward via the super-Alfvénic jet. The laterally expanding exhaust, through which the majority of the electrons exit, allows reconnection to be fast. The observed reconnection rate, deduced in four different ways, was in the range of $7-9\%$, confirming that reconnection was indeed fast in this event. Our observations provide important experimental confirmation that an elongated, super-Alfvénic, and unfrozen electron jet is produced as a consequence of fast reconnection. More importantly, the observations establish a minimum length of the jet or diffusion region, which far exceeds what is seen in current simulations.

The observed elongated electron jet in the middle of the current sheet is different from most of the previously reported electron-scale layers which were located along separatrices [15,16]. Nevertheless, these previous studies also indicated that electron-scale physics extends far from the inner electron diffusion region.

We thank the Cluster FGM and CIS teams for providing the magnetic field and plasma data. This research was supported by NSF, NASA, and DOE.

[1] M. A. Shay and J. F. Drake, Geophys. Res. Lett. **25**, 3759 (1998).
[2] M. Hesse *et al.*, Phys. Plasmas **6**, 1781 (1999).
[3] P. L. Pritchett, J. Geophys. Res. **106**, 3783 (2001).
[4] W. Daughton *et al.*, Phys. Plasmas **13**, 072101 (2006).
[5] M. A. Shay *et al.*, Phys. Rev. Lett. **99**, 155002 (2007).
[6] H. Karimabadi *et al.*, Geophys. Res. Lett. **34**, L13104 (2007).
[7] T. D. Phan *et al.*, Geophys. Res. Lett. **34**, L14104 (2007).
[8] B. U. Ö. Sonnerup, in *Solar System Plasma Physics*, edited by L. J. Lanzerotti, C. F. Kennel, and E. N. Parker (North Halland Pub., Amsterdam, 1979), Vol. 3, p. 46.
[9] M. E. Mandt *et al.*, Geophys. Res. Lett. **21**, 73 (1994).
[10] T. Nagai *et al.*, J. Geophys. Res. **106**, 25929 (2001).
[11] M. Øieroset *et al.*, Nature (London) **412**, 414 (2001).
[12] F. S. Mozer, *et al.*, Phys. Rev. Lett. **89**, 015002 (2002).
[13] A. Vaivads *et al.*, Phys. Rev. Lett. **93**, 105001 (2004).
[14] M. A. Shay *et al.*, J. Geophys. Res. **103**, 9165 (1998).
[15] F. S. Mozer, J. Geophys. Res. **110**, A12222 (2005).
[16] F. S. Mozer *et al.*, Geophys. Res. Lett. **32**, L24102 (2005).